Macromolecules

ARTICLE

pubs.acs.org/Macromolecules

Monitoring in Real-Time the Degrafting of Covalently Attached Fluorescent Polymer Brushes Grafted to Silica Substrates—Effects of pH and Salt

Olga Borozenko,[†] Robert Godin,[‡] Kai Lin Lau,[†,‡] Wayne Mah,[‡] Gonzalo Cosa,[*,‡] W. G. Skene,[*,†] and Suzanne Giasson[*,†]

[†]Department of Chemistry Université de Montréal, C.P. 6128, succursale Centre-Ville, Montréal, QC, Canada, H3C 3J7

[‡]Department of Chemistry, McGill University, 801 Sherbrooke Street West, Montreal, QC, Canada, H3A 2K6

Supporting Information

ABSTRACT: Poly(acrylic acid) (PAA) covalently immobilized on glass substrates was made fluorescent by grafting a BODIPY derivative (PMOH) via an ester linkage. Although only nanograms/square centimeter of polymer are understood to be immobilized onto the SiO_2 substrate, the fluorophore-tagged polymer was readily visible to the naked eye and its fluorescence was easily detected. The characteristic BODIPY emission, centered at 550 nm, was used to follow the degrafting of PAA from the glass substrates in aqueous solution in real-time using total internal reflection fluorescence (TIRF) microscopy. The substrate−initiator bond hydrolysis and the conditions at which the PAA degrafting occurred were unequivocally confirmed in real-time by TIRF microscopy. No cleavage of the polymer occurred between pH 6.5 and 10.5 in the absence of NaCl. In contrast, polymer degrafting from the substrate occurred at pH ≥ 9.5 when 10 mM NaCl was added to the buffer solution.

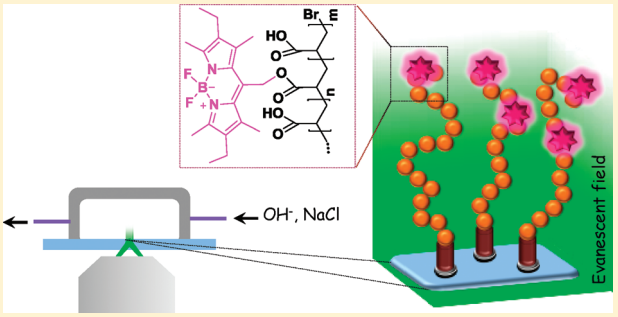

INTRODUCTION

Polymer-bearing surfaces are of particular interest because of their thermal and solvent response,[1,2] their prospective use as protein and cell adhesive platforms,[3−5] or as self-biolubricating substrates, among others.[6] Surface-tethered polymer chains provide the means to tailor the surface properties by undergoing externally stimulated conformational changes. This is particularly true for polyelectrolyte polymers such as poly(acrylic acid) (PAA) whose degree of ionization is highly influenced by pH, ionic strength, and the presence of multivalent species.[7,8] Various polymer conformations including pancake and brushes are possible with end-tethered polyelectrolytes by varying surface density and the media.[9] The control of conformational properties have allowed for advances in areas such as surface friction modulation, switchable wettability, autophobicity,[10−12] antifouling[13−16] and lubricity,[6,17−21] to name but a few.

Surface-bound polymers of well-defined discrete degrees of polymerization and high surface homogeneity are desired for ensuring control of surface properties and reversible surface response with external stimuli such as temperature, pH and ionic strength. These polymers can be obtained by controlled polymerization with an ATRP initiator chemically linked to the substrate. For silica substrates, the substrate−initiator linkage ($Si_{substrate}$−O−$Si_{initiator}$ bond) is generally robust enough for both sustaining the reaction conditions required for ATRP and subsequent polymer brush formation and characterization. We recently showed that PAA brushes built on mica by anchoring polystyrene-poly(acrylic acid)(PS-*b*-PAA) diblock copolymers in a polystyrene monolayer covalently attached to OH-activated mica surfaces resist to cleavage at pH 5.5 with added salt for several days.[22] However, there is still uncertainty regarding the robustness of the substrate−polymer bond and whether it is resistant to the extreme pH and ionic strengths that are required for conformational analyses of polyelectrolyte brushes. It is unknown whether these extreme conditions hydrolyze the Si−O−Si bond and cleave the polymer from the substrate leading to undesired decrease in polymer grafting density, similar to what was reported for poly(methacrylic acid) brushes and PAA brushes grafted from silica-based substrates.[23−25]

Knowing the conditions under which undesired polymer cleavage occurs is pivotal for accurate surface-property studies. They are also important for controlling reversible polymer conformational changes, while preventing polymer degrafting. Although we previously provided indirect evidence for polymer cleavage from mica at high pH and salt concentrations,[23] determining the exact conditions under which PAA cleavage occurred was not possible. Also, unequivocal evidence for polymer degrafting from silica substrates has not yet been demonstrated.

Received: June 17, 2011
Revised: August 23, 2011
Published: September 22, 2011

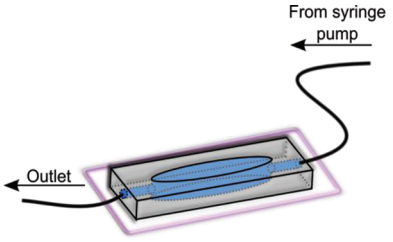

Figure 1. Flow-through chamber of a silicon elastomer mounted on the glass coverslip bearing the PMOH−PAA.

Therefore, direct evidence for polymer degrafting and the conditions under which it occurs on glass substrates is of importance for accurate structure−property studies.

Motivated by the need to unequivocally confirm polymer cleavage from silica substrates and to determine the exact pH and ionic conditions at which the undesired cleavage occurs, we explored a number of techniques to follow this process, including AFM and ellipsometry. On one hand, AFM is a sensitive method for accurate step-height measurements for micrometer-sized areas, the low scan rate and limited sample area however preclude the analyses of multiple samples for accurately assessing the degrafting conditions in solution. It is also a static analytical tool requiring the samples to be equilibrated in the given solution prior to analyses. Therefore, detecting the real-time degrafting in solution is not possible. On the other hand, rapid surface analyses over larger areas are possible by ellipsometry. However, direct quantitative measurements in solution under various conditions are problematic owing to local variations in refractive indices with changes in pH and salt concentration.

Total internal reflection fluorescence (TIRF) microscopy is an ideal method for studying the degrafting of covalently linked polymer brushes from silica surfaces and it is a suitable alternative to AFM and ellipsometry. The evanescent field achieved in total internal reflection enables selective excitation of the region in close proximity (tens to hundreds of nanometers) to the surface resulting in strong signals with low background emission.[26,27] Labeling of the otherwise nonemissive PAA would make it compatible with TIRF microscopy usage while providing the sensitivity required for detecting the subng polymer quantities grafted on the substrate. An additional advantage of TIRF microscopy is that multiple samples of various medium conditions can be tested on a single silica substrate, therefore minimizing the variability in grafting density, surface roughness, and other inherent inconsistencies between different substrates. By far, the main advantage of this technique is that solutions of desired pH and salt concentration can be flowed directly over the substrate during the fluorescence measurements (Figure 1). Therefore, the pH and ionic strengths required for polymer degrafting can be directly obtained in real-time by monitoring the fluorescence decrease as a function of the media being flowed over the substrate.

Although TIRF microscopy is well-suited for studying the degrafting of PAA from silica substrates in real-time and is advantageous relative to other techniques, the polymer must be fluorescent. As a result, we herein report the preparation of a fluorescently tagged PAA and the use of TIRF microscopy for unequivocally confirming polymer degrafting from glass substrates. The pH and salt conditions required to promote polymer cleavage from the substrate are presented.

EXPERIMENTAL SECTION

Materials. Chemicals were used as received from Aldrich unless otherwise stated. Copper bromide (CuBr) was purified as previously reported.[28] *tert*-Butyl acrylate (*t*BA) and styrene were purified by passing through a column of basic alumina, followed by vacuum distillation immediately prior to use. 8-Acetoxymethyl-2,6-diethyl-1,3,5,7-tetramethyl pyrromethenefluoroborate (PM 605) was purchased from Exciton, Inc. (Dayton, OH). Milli-Q water was taken from a Millipore grade A 10 purification system. Silicon wafers were obtained from University Wafer Co. All glassware was oven-dried at 120 °C overnight. Glass coverslips (Fisherbrand No. 1) for TIRF microscopy experiments were purchased from Fisher Scientific.

8-Hydroxymethyl-2,6-diethyl-1,3,5,7-tetramethylpyrromethene Fluoroborate (PMOH). PMOH was prepared from its commercially available ester (PM 605) following previously reported methods.[29−32]

Substrate Preparation and Initiator Immobilization. Glass slides (22 × 22 mm^2) were cut in half using a diamond pencil. The glass substrates were treated with a Piranha solution (Caution!) (H_2SO_4/H_2O_2 70:30 v/v) for 15 min for removing organic residues and for silanol activation. The activated surfaces were then rinsed with water and ethanol and dried under a gentle stream of nitrogen. The initiator, 3-(chlorodimethylsilyl)propyl-2-bromoisobutyrate synthesized according to known means,[28] was dissolved in anhydrous toluene (1 mM).[28] Functionalization of one side of the substrate was done by covering the top side of the slide with a drop of the initiator solution. The solution was allowed to react for 15 min at room temperature after which, the slides were sequentially washed with toluene, absolute ethanol, and Milli-Q water. They were dried with nitrogen and used immediately for surface-initiated polymerization.

Silicon wafers were cut to 12 × 22 mm^2 pieces and treated with Piranha solution for 15 min. The substrates were then washed thoroughly with Milli-Q water and absolute ethanol, dried under nitrogen and placed in a compartmentalized reactor containing the initiator (1 mM) that was dissolved in anhydrous toluene.[28] After 17 h, the substrates were removed from the reactor, rinsed with toluene, absolute ethanol, Milli-Q water, and then dried under nitrogen. The substrates were stored in a vacuum desiccator until used.

Surface-Initiated Polymerization of *tert*-Butyl Acrylate (*t*BA) with Added Free Initiator. Polymerization of the *t*BA on the initiator-functionalized glass substrates was carried out as previously reported.[33] Residual physisorbed polymers on the glass slides were removed by Soxhlet extraction with THF for 8 h. The slides were stored in a desiccator until used. The resulting polymerization solution was diluted with acetone and passed through a column of neutral alumina for removing the copper salts. The polymer solution was then concentrated in vacuo and the molecular weight was determined by GPC with the appropriate concentration in THF.

Surface-Initiated Polymerization of Styrene with Added Free Initiator. Freshly distilled styrene and acetone were deoxygenated under argon for 1 h. CuBr (30 mg, 2 × 10^{-4} mol) was placed into a 50 mL double-necked round bottomed flask. The flask was degassed under vacuum at room temperature and backfilled with argon three times. Deoxygenated styrene (9.2 mL, 8 × 10^{-2} mol), deoxygenated acetone (4.6 mL), and hexamethyltriethylenetetramine (HMTETA) (100 μL, 4 × 10^{-4} mol) were added to CuBr, and the mixture was stirred at room temperature under argon until a homogeneous green solution was obtained. A clean initiator functionalized glass slide was placed in a flame-dried Schlenk flask, which was deoxygenated under vacuum and backfilled with argon three times. The above-described polymerization solution was transferred into the reaction flask followed by injection of ethyl-2-bromoisobutyrate as the free initiator (30 μL, 2 × 10^{-4} mol). The flask was heated at 65 °C for 48 h with stirring. The Schlenk flask

was then placed in a cold bath and the solution was diluted with acetone. The surface was removed and cleaned thoroughly with THF, acetone, and absolute ethanol and dried under stream of nitrogen. A Soxhlet extraction in THF was used for 8 h for removing any physisorbed polymer. The bulk reaction mixture was passed through a column of neutral alumina to remove the catalyst. The solvent was then evaporated and the polymer molecular weight was determined by GPC.

Hydrolysis of Surface-Grafted Poly(*tert*-butyl acrylate) (P*t*BA) to PAA. *tert*-Butyl ester cleavage was done by treating the P*t*BA−grafted glass slides with trifluoroacetic acid (dichloromethane/TFA 10:1 v/v) at room temperature with stirring overnight. The glass substrates were then washed repeatedly with absolute ethanol and Milli-Q water, and then dried under a nitrogen stream.

Coupling of PMOH to PAA. PMOH (20 mg), 1-ethyl-3-(3-(dimethylamino)propyl)carbodiimide hydrochloride (EDCI; 60 mg), and 4-(dimethylamino)pyridine (DMAP; 60 mg) were dissolved in anhydrous dichloromethane (20 mL) in a 100 mL double neck round-bottom flask. PAA-functionalized glass substrates were placed in a compartmentalized reactor equipped with stir bar. The above-prepared solution was transferred to the reactor by cannula and the mixture was then stirred at room temperature for 4 h under argon. The slides were removed from the reaction mixture, washed sequentially with dichloromethane, acetone, absolute ethanol, Milli-Q water and then dried under a nitrogen stream. The physisorbed PMOH was removed by Soxhlet extraction with dichloromethane for 8 h. The fluorophore containing slides were analyzed by UV−vis absorption and fluorescence.

Degrafting of PAA. Trizma base buffer solution (0.1 M) was prepared with Milli-Q water and the pH was adjusted to 6.5, 7.5, 8.5, 9.5, and 10.5 with different volumes of HCl (0.1 M). The pH was measured with a Symphony SB20 pH meter with Ag/AgCl electrode. The ionic strength was varied by adding NaCl (10 mM) to the Trizma buffer solution. The buffer solution of the given pH was flowed over the polymer−substrates during imaging.

SURFACE CHARACTERIZATION

Contact Angle Measurements. Measurements were carried out using an FTA200 dynamic contact angle analyzer (First Ten Angstrom) in the equilibrium static mode, using Milli-Q water as the probe liquid. Data analyses were performed using Fta32 Video software and three separate measurements were done for each glass substrate. The average contact angle value was determined within an experimental precision of ±3°. The empirical Cassie−Baxter equation and modified related equations[34,35] were used to evaluate the relative surface density (or surface coverage) of grafted molecules on the glass surface. These equations correlate the equilibrium contact angle (θ_{obs}) of a chemically heterogeneous surface to the surface coverage of the different molecules on the surface and predict an increase in water contact angle with an increase in surface coverage of small hydrophobic molecules:

$$[1 + \cos(\theta_{obs})]^2 = f_1[1 + \cos(\theta_1)]^2 + f_2[1 + \cos(\theta_2)]^2$$
$$f_1 + f_2 = 1 \quad (1)$$

The water contact angle of a surface covered with a maximum number of hydrophobic molecules, $f_1 = 1$, is presumed to be $\theta_1 = 90$, and the water contact angle of uncovered glass surface, $f_2 = 1$, is $\theta_2 = 0$.

AFM Measurements. The dry thickness of all samples was measured before and after TIRF measurements at room temperature (Figure S4, Supporting Information). The samples were left in Milli-Q water at least 2 h, rinsed with absolute ethanol, dried with nitrogen and the step-height measured by AFM film. The AFM was equipped with a NanoScopeV extended controller and a MultiMode microscope (Digital Instruments, Santa Barbara, CA). All AFM images were collected in the tapping mode using an Arrow-NCR silicon probe with a spring constant of 42 N/m and a resonance frequency of 300 kHz (Nanoworld). Data analyses were performed using the NanoScope 7.30 software. A scalpel was used to scratch and expose the bare slide and step-height between the native glass and the PAA layer was measured in the dry state by an AFM cross sectional height image. The thickness of each sample was measured at three different regions.

Ellipsometry Measurements. Experiments were conducted using an Ellipsometer M-2000 V from J.A. Woollam Co. in air at an incident angle of 75° and a wavelength range of 370−1000 nm. Four independent measurements at different areas were done for each sample.

Ensemble Characterization. The absorption measurements were done on a Cary-500 spectrometer and the fluorescence studies were performed on an Edinburgh Instruments FLS-920 fluorimeter by exciting at 520 nm. Fluorescence experiments in micelles were performed on a PTI Quantamaster 40 equipped with a Quantum Northwest TC 425 temperature controller (at 20°C) by exciting at 500 nm.

TIRF Microscopy. The PMOH-functionalized surface-grafted polymers were imaged using a wide-field objective-based total internal reflection (TIRF) microscopy setup consisting of an inverted microscope (IX71, Olympus) equipped with a laser-based TIRF illumination module (IX2-RFAEVA-2, Olympus).[35,36] Laser excitation was provided by a 25 mW, 532 nm output, diode-pumped cw laser (CL532−025-S, CrystaLaser), attenuated with metallic ND filters and providing 2−7 μW output at the objective. The excitation beam was directed to the sample by reflection on a dichroic beamsplitter (z532rdc) and focused on the back focal plane of a high numerical aperture (N.A. = 1.45) oil-immersion objective (Olympus PLAN APO 60X). Images were additionally magnified 2-fold via an internal lens and a relay lens system and then captured on a back illuminated electron multiplying charge-coupled device (EMCCD) camera (Cascade II:512B, Roper Scientific) using gains between 3700 and 4095 and frame exposure times of 0.6 to 1.5 s. Laser and camera settings were adjusted for each sample in order to obtain initial fluorescence intensities of ca. 120 A.U., while minimizing laser-induced photobleaching. The original 66 × 66 μm^2 TIRF images were cropped to half of the size, corresponding to the reflected channel from a 640dcxr dichroic mirror (<640 nm) in a two color emission setup. To further minimize photobleaching in areas of interest (AOI), images were focused on a subsection of the sample area (round dark regions near middle of images) using an iris positioned in the excitation laser beampath. Image acquisition was started with this iris closed, which was then fully opened during the acquisition. Each image was acquired after repositioning the sample in a new, non illuminated region to minimize photobleaching of the AOI.

TIRF Image Analyses. From the captured movies, the first complete frame in which the iris is fully opened was selected from the others and then further analyzed with the Image Pro 5.1 software. The image analyses consisted of first selecting an AOI to ignore the photobleached focus point as well as consistently darker edges. A histogram of individual pixel intensities was constructed for all of the pixels contained in the AOI (ca. 70 000 pixels, corresponding to a sample area of ca. 1200 μm^2). The histograms were then fitted to a Gaussian function in order to extract the center of the fluorescence intensity distribution. When multiple images were taken within 5 min of each other,

Scheme 1. Schematic Representation of PMOH Coupling to Immobilized PAA To Afford the Fluorescent Polymer, PAA−PMOH

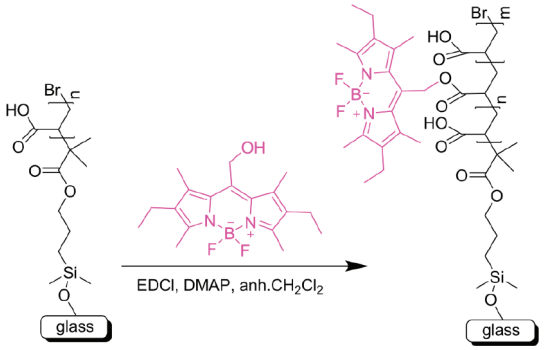

only the averaged center of the distribution was reported and the errors bars corresponding to the standard deviation were added.

TIRF Sample Chamber. Polymer-functionalized glass coverslips were typically washed with dichloromethane and ethanol prior to use. Flow chambers were assembled by depositing a homemade silicone gasket on the glass substrate. These gaskets were designed to have a narrow chamber with an inlet and an outlet holes for inserting the flow tubing. Chambers were fabricated using SYLGARD 184 Silicone Elastomer Kit (Dow Corning Corporation). The undersized glass substrates (ca.12 mm × 22 mm) were then affixed to flat metal plates, which served as the sample holder. The chambers were closed by pressing a clean, blank coverslip on top of the gasket. The sample chambers had internal volumes of ~50 μL. Solutions of known pH and NaCl concentration were continuously flowed at a rate of 1 μL/min over the substrate using a syringe pump system for periods of 2 h or more. One freshly prepared PAA-PMOH covered glass slide for each buffer solution at a given pH and ionic strength was analyzed.

RESULTS AND DISCUSSION

Fluorescent Monomer Synthesis. PMOH (Scheme 1) was prepared according to known means.[31] This was the chosen fluorophore because its spectroscopic properties are well-known and its alcohol derivative could be coupled to the immobilized PAA according to standard coupling protocols. This would afford the required fluorescent polymer for TIFR measurements.[37,38] The advantage of PMOH over other dyes is that it has a strong absorption extinction coefficient, narrow fluorescence emission, high emission quantum yield, and photochemical stability.[37,39−41] These properties make it possible to detect the subng quantities of the polymer immobilized on the glass substrates (Figures S1 and S2, Supporting Information).

Fluorescent Polymer Synthesis. Immobilization of a uniform initiator layer was carried out on only one side of the spectroscopically transparent silica surface, specifically the one in contact with the aqueous solutions. This is necessary to avoid background fluorescence from the layer not in contact with the flow solution. Contact angle measurements were done for confirming initiator grafting to the substrate. The measured contact angle of θ_{water}= 72° (Table 1) is in agreement with our previous results[28,33] and confirms that the initiator is coupled to the substrate in comparison to Piranha-solution treated native glass slides whose contact angle is 0°. The equilibrium contact angle of a chemically heterogeneous surface can be related to the fraction of the initiator groups in terms of the phenomenological modified Cassie−Baxter equation (eq 1). According to this equation, a contact angle of 72° corresponds to a surface coverage value of 76% (Table 1). The surface density of end-grafted polymers synthesized using the *graft from* method inherently depends on the initiator grafting density.

Controlled surface polymerization was subsequently done with the failsafe ATRP of *t*BA using ethyl-2-bromoisobutyrate as free initiator. Following polymerization at 60 °C for 15 h, the water contact angle measured was 83° (Table 1). Controlled polymerization was confirmed by the linear increase in both the polymer layer thickness and the average molecular weight of free-polymer in solution. The trend provides indirect evidence that polymer degrafting does not occur under the polymerization conditions, otherwise both variable film thickness and variable molecular weight of the free-polymer in solution would be observed. The molecular weight of the free polymer, relative to polystyrene standards, was determined by GPC. The grafting density σ of the PtBA layer was calculated from the dry polymer thickness d ($\sigma = d\rho N_A/M_n$ where ρ is the density of PtBA (1.047 g·cm^{-3})), N_A is Avogadro's number, and M_n is the number average molecular weight of the grafted polymer chains which is assumed to be similar to that of the free polymer in solution (60 326 g/mol). We use this assumption because it was not possible to determine the molecular weight of the very small amount of generated grafted chains. It has been shown that the molecular weight of the grafted polymer grown by ATRP can be similar to or slightly larger than the molecular weight of free polymer in solution.[43,44] High grafting density of 0.41 chain/nm^2 was found (Table 1). The distance between two adjacent grafted end-groups can be estimated as $s = 1/\sigma^{1/2}$ = 1.56 nm and compared to the characteristic size of the chains in order to evaluate the conformation of the chains. As the polymer layer is in a dry state, we assumed that the grafted chains adopt a collapsed state with a characteristic dimension R = 1.95 nm ($R \approx aN^{0.33}$, where a is a characteristic dimension of repeating unit, 0.25 nm)[42] and N is the average number of repeating units of the PtBA chains which is assumed to be the same as that of the free polymer chains in solution, i.e., 471. Pancake and mushroom conformations are specific to polymer chains tethered at low grafting density (or $s > R$) while the brush conformation prevails at high grafting density (or $s \ll R$).[45] Our results (s slightly smaller than R) suggest that the grafted chains adopt a conformation at the frontier between the brush and mushroom conformations. An underestimation of molecular weight for the attached polymer chains would result in a smaller polymer grafting density σ for a given polymer layer thickness d, or a larger distance between grafted chains s, and therefore, the chains would adopt a mushroom conformation. However, in a good solvent or when ionized, the collapsed grafted chains are expected to stretch into a brush conformation for a given grafting density and chain length.[45,46]

Removal of the *tert*-butyl deprotecting group was carried out by refluxing the polymer-immobilized glass substrates in trifluoroacetic acid/dichloromethane,[47] resulting in a decrease in the water contact angle to θ_{water} = 35°. PMOH was subsequently coupled to PAA with EDCI to afford the fluorescent polymer, PAA−PMOH (Scheme1). Covalent coupling of PMOH to the immobilized PAA was spectroscopically confirmed by the characteristic absorbance and fluorescence of the PMOH ester, which peaked at 550 and 564 nm, respectively (Figure 2). The surfaces were then washed via Soxhlet extraction in dichloromethane for 8 h in

Table 1. Surface Properties of Initiator-Functionalized and PAA-Functionalized Silica Substrates

		polymer layer					
initiator layer		PtBA				PAA	
θ_{water} (±2°)	f_1	θ_{water} (±2°)	dry thickness (±2 nm)[a]	M_n(g·mol^{-1})	σ^b (chain/nm^2)	θ_{water} (±2°)	dry thickness (±4 nm)[a]
72	0.76	80	40	60 326	0.41	35	14

[a] The thickness was measured by AFM step height method. [b] $\sigma = (d\rho N_A)/M_n$ where d is the dry layer thickness, ρ is the density of PtBA (1.047 g cm^{-3}), N_A is the Avogadro's number, and M_n is the average molecular weight of the grafted polymer chains and it is similar to the M_n of the free polymer.

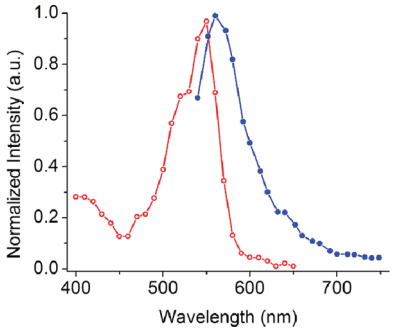

Figure 2. Normalized absorption (red ○) and emission (blue ●) spectra (λ_{ex} = 520 nm) of immobilized PAA−PMOH on silica slides.

order to remove any potentially physisorbed PMOH. Neither the absorbance nor fluorescence intensity changed after Soxhlet extraction, confirming covalent attachment of the PMOH to the polymer and covalent attachment of the polymer to the silica substrate.

PMOH was grafted to the immobilized PAA layer in low amounts in order to ensure fluorimetric visualization of the polymer layer while minimizing polymer insensitivity toward both variations in pH and salt concentration arising from fluorophore tagging on every repeat unit. Also of note is the direct polymerization of AA-PMOH by ATRP on initiator-covered silica substrate that was attempted according to standard methods.[48] Unfortunately, no polymer could be detected either in solution or on the surface. Subsequently, direct polymerization of AA (acrylic acid) using modified ATRP protocols was pursued. Although AA could be polymerized from the surface in water, the control of film thickness is relatively difficult to obtain because of fast polymerization kinetics[49] and hydrolytic side reactions occurring in aqueous media.[24] Indeed, the variable polymer thickness (between 10 and 120 nm) despite consistent polymerization conditions, confirms that the surface polymerization of AA is not controlled and that PAA is most likely cleaved from the substrate under the ATRP polymerization conditions of high pH (pH > 8) and salt concentration required for AA (vide infra).

TIRF Microscopy Degrafting Studies. Fluorescence from the PMOH−PAA immobilized on glass substrates was observed when immersing the substrates in aqueous solutions of increasing pH when excited with the TIRF system. The laser power transmitted through the objective was attenuated to 2−7 μW for minimizing any PMOH photobleaching during the experiments. The top surface, to which was grafted the PMOH−PAA, was adapted with a ca. 50 μL volume flow chamber for both exposing the polymer layer to a constant flow of desired solution and washing away any degrafted polymer (Figure 1).

Figure 3 displays typical fluorescence images of a 66 × 33 μm^2 region obtained at close to neutral pH (pH = 6.5, top left panel A)

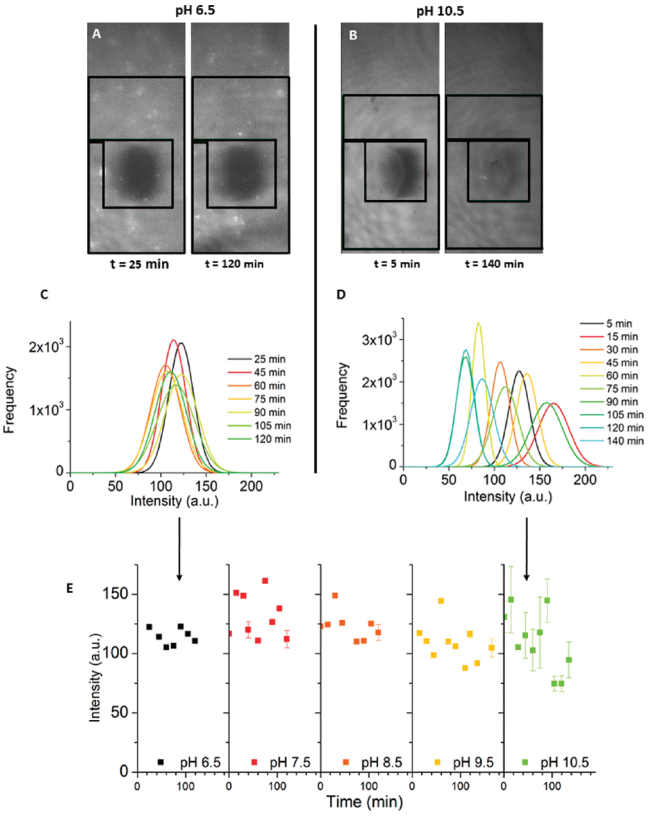

Figure 3. Time-dependent PMOH−PAA fluorescence as a function of pH with no added NaCl. (A and B) TIRF images of substrates after flowing at low (A) and high pH (B) NaCl-free solutions for increasing amounts of time. (C and D) Time evolution of Gaussian-fitted individual pixel fluorescence intensity distributions when flowing at low (C) and high pH (D) NaCl-free solutions. (E) Center of Gaussian-fitted pixel fluorescence intensity distributions versus time for all the salt-free solutions studied. The analyzed area is delimited by the square and rectangle on the corresponding picture.

and high pH (pH =10.5, top right panel B). The images were obtained shortly after initial exposure and following long exposure to the NaCl-free buffer solution. Images with smooth intensity profiles were observed, confirming the homogeneous distribution of the PMOH−PAA layer across the slide. Intensity variations of ca. 10% were observed for a given sample as a result of different regions being monitored (see for example Figure 3E, pH 6.5 or 7.5) and variations in the laser power. The intensity of a subregion (delimited by the rectangle and square in Figure 3, A and B) was further analyzed to indirectly quantify surface density of the immobilized polymer over time. The histogram of the intensity per pixel was obtained for a given pH with increasing exposure

dx.doi.org/10.1021/ma2013755 |Macromolecules 2011, 44, 8177–8184

times to the solution (Figure 3, parts C and D). New regions in the same substrate were then imaged at each time delay for minimizing PMOH photobleaching followed by plotting the intensity/pixel value at the center of the Gaussian-fitted histogram vs time (bottom panel E, Figure 3). It is obvious from the statistically analyzed data graphically summarized in Figure 3E that no polymer degrafting occurs regardless of pH at low ionic strength.

Polymer degrafting at a high ionic strength was next investigated as a function of time and pH (Figure 4) with a NaCl concentration of 10 mM. Although the monovalent salt was not expected to directly promote polymer cleavage,[50,51] it however can increase the degree of dissociation of PAA leading to polymer backbone extension with increasing density of negative charges.[51,52] The expected

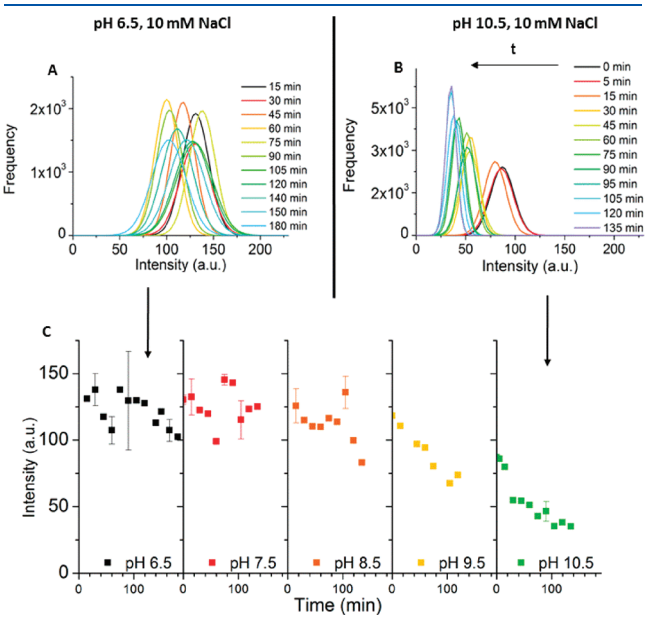

Figure 4. Time and pH dependence of PMOH−PAA degrafting at 10 mM NaCl. (A and B) Time evolution of Gaussian-fitted individual pixel fluorescence intensity distributions when flowing at low (A) and high pH (B) with 10 mM NaCl. (C) Center of Gaussian-fitted pixel fluorescence-intensity distributions versus time for all solutions studied at 10 mM NaCl.

extended conformation in turn exposes the substrate−initiator bond to hydroxyl ions, which potentially promotes degrafting. As shown in Figure 4C, the fluorescence intensity of the grafted PMOH−polymer is unchanged at pH values ranging from 6.5 to 8.5, but decreases only at pH 9.5 and 10.5. The results confirm that the substrate−initiator bond is labile and can be hydrolyzed resulting in cleavage of the immobilized polymer from the substrate. However, the exact location (within the initiator) where bond rupture occurs is unknown because the C−O, Si−O, Si−C bonds are all potentially labile and susceptible to hydrolysis. Our results further suggest that the substrate−initiator bond is protected against hydrolysis at low ionic strength most probably because of the collapsed conformation of polymer segments close to the surface. However, at extreme pH with added salt, the end-grafted chains are ionized resulting in an extended brush conformation that exposes the substrate−initiator bond making it more susceptible to hydrolysis by hydroxyl ions.

AFM step-height cross-sectional measurements (Figures 5 and S4 (Supporting Information)) were done before and after the TIRF measurements to ensure that the disappearance of the fluorescence signal was due to polymer cleavage and not from either fluorophore cleavage from the polymer or fluorophore quenching processes. The step-height analysis revealed a drastic change in polymer film thickness for the substrates exposed to 10 mM NaCl at pH 10.5 (Figure 5, C and D). This is in contrast to the polymer thickness that remained unchanged before and after exposing to pH 10.5 without added salt (Figure 5, A and B). The height difference between the bare substrate and the polymer layer can quantitatively be determined from the AFM step-height measurements. The degrafting ratio, defined as the ratio between the polymer layer thickness after and before exposure to buffer solution, is ca. 0.2 for the substrate exposed to pH 10.5 with added salt. This suggests that about 80% of the polymer is cleaved from the substrate. Similarly, 40% of the polymer is degrafted from the substrate exposed to pH 9.5 with added salt (Figure 6). Conversely, no polymer degrafting was observed by AFM for the substrate exposed to pH 9.5 without salt. The AFM results corroborate the TIRF measurements in that polymer degrafting occurs only in the presence of salt at pH ≥ 9.5.

Further confirmation that the observed change in fluorescence intensity arises from polymer degrafting rather than hydrolysis of

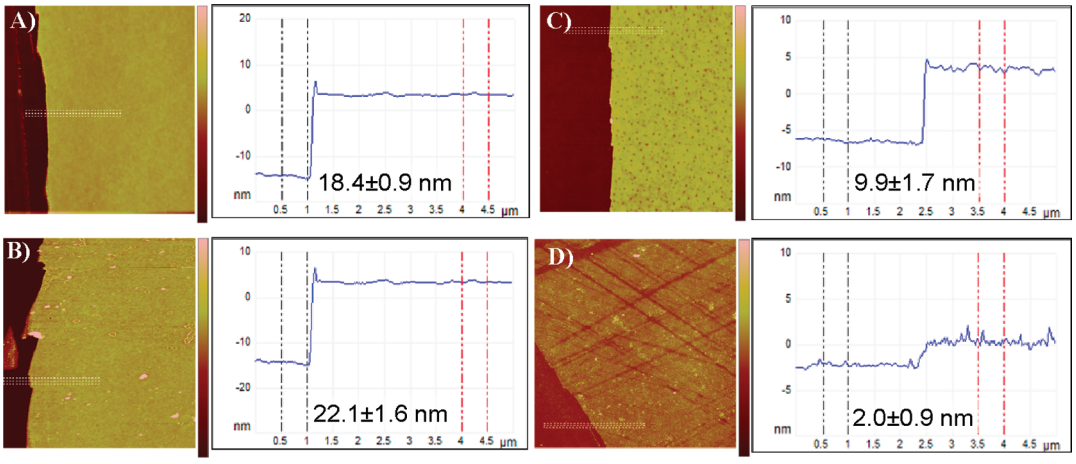

Figure 5. AFM images (10 × 10 μm) in the dry state showing the step-height difference between the bare glass and the polymer layer: (A) before and (B) after exposing the substrate to buffer solution at pH 10.5 and (C) before and (D) after exposing the substrate to buffer solution at pH 10.5 with added salt. The dashed rectangles (0.3 × 5 μm) refer to the step-height analyzed areas.

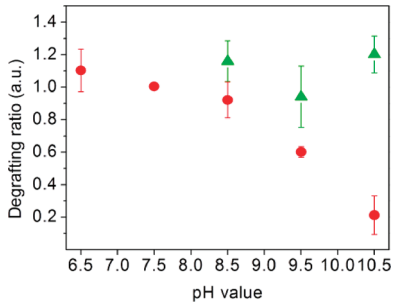

Figure 6. Average PMOH−PAA polymer degrafting ratio taken as the ratio between the polymer layer thickness after and before exposing the substrates to different pH without (green ▲) and with (red ●) added salt. Three different ratios were obtained for each substrate and the standard deviation was used as the error bar.

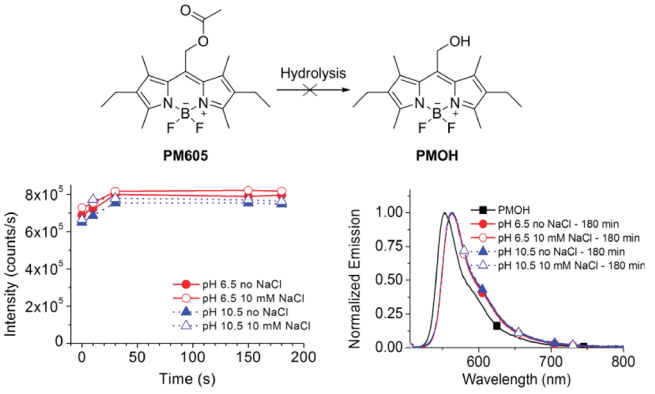

Figure 7. Fluorescence emission spectra of PM605 and PMOH in sodium dodecyl sulfate (SDS, 10 mM) micelles and Trisma (0.1 M) buffer solution. Left: Fluorescence intensity acquired at the emission maximum of PM605 following various incubation periods in aerated solutions at pH 6.5, at 0 and 10 mM NaCl (red, closed and open circles, respectively), and pH 10.5 at 0 and 10 mM NaCl (blue, closed and open triangles, respectively). Right: Normalized steady-state fluorescence spectra at various pH and NaCl concentrations after incubation for 180 min. The spectra of PMOH, (which is blue-shifted with respect to PM605), is shown for comparison illustrating that no ester hydrolysis and formation of PMOH occurs during this time period. Excitation was performed at 500 nm in all experiments.

the PMOH−PAA bond was obtained by studying the fluorescence of a PMOH−PAA model system, PM605 in SDS micelles. The hydrolysis of PM605 to PMOH (inset top Figure 7) would give rise to a hypsochromic shift in the fluorescence emission (right panel Figure 7).[29−31,39,53,54] No change in either the emission spectrum shape or intensity was observed upon incubating PM605 for extended periods of time in solutions of pH and ionic strength similar to those used for the TIRF microscopy studies. Only a slight fluorescence increase was observed at 564 nm at the onset of the measurement because of PM605 diffusing into the micelles. In contrast, hydrolysis of PM605 would result in a decrease in intensity at 564 nm. The steady-state emission intensity vs time analyses of PM605 in SDS micelles confirm that ester hydrolysis or bleaching of the dye do not occur. The results further confirm that the fluorescence decrease observed in TIRF microscopy is a result of PAA degrafting from the substrate and not from PMOH hydrolysis.

The degrafting rate can be estimated from the time-dependent fluorescence change in Figure 4C. The degrafting rate for pH 9.5 and 10.5 with added NaCl is approximately the same. The lack of sensitivity of the degrafting rate to $[OH^-]$ and the sudden onset of degrafting can be interpreted by a change in polymer conformation when the pH is increased close to 9.5 at high ionic strengths. Although, the $[OH^-]$ is expected to be sufficient to induce polymer degrafting at pH < 9.5, the polymer conformation is tightly collapsed at low ionic strength and protects the labile substrate−initiator bond. A combination of high pH and high ionic strength are thus needed to induce the conformation change of grafted PAA. These results are in good agreement with our previous study showing conformation change of PAA brushes with pH and salt.[23]

In order to protect the labile substrate−initiator bond at the polymer/substrate interface from undesired hydrolysis, a hydrophobic layer can be inserted between the substrate and the PAA as similarly done with a PS-*b*-PAA copolymer grafted to mica.[22] The presence of the innermost hydrophobic layer directly bond to mica is expected to act as a protective layer against hydrolysis of the substrate−initiator bond by preventing water and hydrated ions from reaching the substrate. Therefore, we have grafted a polystyrene layer directly from the glass substrate using the immobilized ATRP initiator as in Figure 2. The thickness of the grafted polystyrene layer measured by ellipsometry was 10 nm. The substrate was then exposed to pH 10.5 solution for 2.5 h and then cleaned. No change in the polymer film thickness was observed by ellipsometry regardless of ionic strength, confirming that the polystyrene layer can provide a robust layer or spacer protecting the labile substrate−initiator bond against hydrolysis. As the PS chains contain a terminal bromine, they allow for subsequent polymerization of AA by ATRP block copolymerization. This is actively being pursued.

CONCLUSION

Degrafting of covalently immobilized fluorescent PAA from glass substrates was unequivocally confirmed in solution via TIRF microscopy. The real-time fluorescence measurements confirm that the substrate−initiator bond is labile and can be cleaved. Cleavage of the covalently bound polymer only occurred at pH ≥ 9.5 in the presence of salt. The combination of high pH and added salt most probably induces a conformational change of the polymer layer, allowing hydrolysis of the substrate−initiator bond at the polymer/glass interface. Although the exact salt and pH induced conformation change is unknown, the hydroxyl ions nonetheless penetrate through the PAA layer to the substrate and hydrolyze the glass−initiator bond. The absence of polymer degrafting with 10 mM NaCl at pH < 9.5 suggests that the polymer adopts a compact conformation close to the surface and protects the glass−initiator bond against hydrolysis. Regardless of conformation, we provided unprecedented real-time evidence for the degrafting of PAA from glass substrates. The stability of the covalently attached hydrophobic−hydrophilic copolymer layer is currently being investigated.

ASSOCIATED CONTENT

Supporting Information. Pictures of PAA−PMOH covered glass slides under ambient and UV light, GPC, and AFMs. This material is available free of charge via the Internet at http://pubs.acs.org.

AUTHOR INFORMATION

Corresponding Author
*E-mail: (G.C.) gonzalo.cosa@mcgill.ca; (W.G.S.) w.skene@umontreal.ca; (S.G.) suzanne.giasson@umontreal.ca.

ACKNOWLEDGMENT

This work was supported by le Fonds de Recherches sur la Nature et les Technologies and the Natural Sciences and Engineering Research Council (NSERC) Canada. W.G.S. thanks both the Alexander von Humboldt Foundation and the RSC for a JWT Jones Travelling Fellowship, allowing this manuscript to be completed. R.G. thanks the NSERC for a postgraduate scholarship; K.L.L. thanks both the Faculty of Science at McGill University and the Centre of Self-Assembled Chemical Structures for undergraduate scholarships. The authors thank Prof. R. Prud'homme for access to AFM.

REFERENCES

(1) Jonas, A. M.; Glinel, K.; Oren, R.; Nysten, B.; Huck, W. T. S. *Macromolecules* **2007**, *40*, 4403–4405.
(2) Aoki, H.; Kitamura, M.; Ito, S. *Macromolecules* **2008**, *41*, 285–287.
(3) Harris, B. P.; Kutty, J. K.; Fritz, E. W.; Webb, C. K.; Burg, K. a. J. L.; Metters, A. T. *Langmuir* **2006**, *22*, 4467–4471.
(4) Jain, P.; Baker, G. L.; Bruening, M. L. *Annu. Rev. Anal. Chem.* **2009**, *2*, 387–408.
(5) Wischerhoff, E.; Uhlig, K.; Lankenau, A.; Borner, H. G.; Laschewsky, A.; Duschl, C.; Lutz, J.-F. *Angew. Chem. Int. Ed* **2008**, *47*, 5666–5668.
(6) Raviv, U.; Giasson, S.; Kampf, N.; Gohy, J.-F.; Jérôme, R.; Klein, J. *Nature* **2003**, *425*, 163–165.
(7) Gong, P.; Wu, T.; Genzer, J.; Szleifer, I. *Macromolecules* **2007**, *40*, 8765–8773.
(8) Wu, T.; Gong, P.; Szleifer, I.; Vlcek, P.; Subr, V.; Genzer, J. *Macromolecules* **2007**, *40*, 8756–8764.
(9) Liu, G.; Yan, L.; Chen, X.; Zhang, G. *Polymer* **2006**, *47*, 3157–3163.
(10) Reiter, G.; Auroy, P.; Auvray, L. *Macromolecules* **1996**, *29*, 2150–2157.
(11) Reiter, G.; Khanna, R. *Langmuir* **2000**, *16*, 6351–6357.
(12) Epps, T. H.; DeLongchamp, D. M.; Fasolka, M. J.; Fischer, D. A.; Jablonski, E. L. *Langmuir* **2007**, *23*, 3355–3362.
(13) Zdyrko, B.; Klep, V.; Li, X. W.; Kang, Q.; Minko, S.; Wen, X. J.; Luzinov, I. *Mater. Sci. Eng. C-Biomimetic Supramol. Syst.* **2009**, *29*, 680–684.
(14) De Giglio, E.; Cometa, S.; Cioffi, N.; Torsi, L.; Sabbatini, L. *Anal. Bioanal. Chem* **2007**, *389*, 2055–2063.
(15) Hollmann, O.; Gutberlet, T.; Czeslik, C. *Langmuir* **2007**, *23*, 1347–1353.
(16) Xu, F. J.; Neoh, K. G.; Kang, E. T. *Prog. Polym. Sci.* **2009**, *34*, 719–761.
(17) Dunlop, I. E.; Briscoe, W. H.; Titmuss, S.; Jacobs, R. M. J.; Osborne, V. L.; Edmondson, S.; Huck, W. T. S.; Klein, J. *J. Phys. Chem. B* **2009**, *113*, 3947–3956.
(18) Zeng, H. B.; Tian, Y.; Zhao, B. X.; Tirrell, M.; Israelachvili, J. *Langmuir* **2009**, *25*, 4954–4964.
(19) Vyas, M. K.; Nandan, B.; Schneider, K.; Stamm, M. *J. Colloid Interface Sci.* **2008**, *328*, 58–66.
(20) Kobayashi, M.; Kaido, M.; Suzuki, A.; Ishihara, K.; Takahara, A. *J. Jpn. Soc. Tribol.* **2008**, *53*, 357–362.
(21) Drummond, C.; Rodriguez-Hernandez, J.; Lecommandoux, S.; Richetti, P. *J. Chem. Phys.* **2007**, *126*, 184901–184912.
(22) Liberelle, B.; Banquy, X.; Giasson, S. *Langmuir* **2008**, *24*, 3280–3288.
(23) Lego, B.; Skene, W. G.; Giasson, S. *Macromolecules* **2010**, *43*, 4384–4393.
(24) Tugulu, S.; Barbey, R.; Harms, M.; Fricke, M.; Volkmer, D.; Rossi, A.; Klok, H.-A. *Macromolecules* **2006**, *40* (2), 168–177.
(25) Wasserman, S. R.; Tao, Y.-T.; Whitesides, G. M. *Langmuir* **1989**, *5*, 1074–1087.
(26) Axelrod, D. *Traffic* **2001**, *2*, 764–774.
(27) Axelrod, D. In *Methods Enzymology*; Gerard, M., Ian, P., Eds.; Academic Press: San Diego, CA, 2003; Vol. 361, pp 1−33.
(28) Lego, B.; Skene, W. G.; Giasson, S. *Langmuir* **2008**, *24*, 379–382.
(29) Khatchadourian, A.; Krumova, K.; Boridy, S.; Ngo, A. T.; Maysinger, D.; Cosa, G. *Biochemistry* **2009**, *48*, 5658–5668.
(30) Krumova, K.; Oleynik, P.; Karam, P.; Cosa, G. *J. Org. Chem.* **2009**, *74*, 3641–3651.
(31) Oleynik, P.; Ishihara, Y.; Cosa, G. *J. Am. Chem. Soc.* **2007**, *129*, 1842–1843.
(32) Amat-Guerri, F.; Liras, M.; Carrascoso, M. L.; Sastre, R. *Photochem. Photobiol.* **2003**, *77*, 577–584.
(33) Lego, B.; François, M.; Skene, W. G.; Giasson, S. *Langmuir* **2009**, *25*, 5313–5321.
(34) Israelachvili, J. N.; Gee, M. L. *Langmuir* **1989**, *5*, 288–289.
(35) Lo, P. K.; Karam, P.; Aldaye, F. A.; McLaughlin, C. K.; Hamblin, G. D.; Cosa, G.; Sleiman, H. F. *Nat Chem* **2010**, *2*, 319–328.
(36) Ngo, A. T.; Lau, K. L.; Quesnel, J. S.; Aboukhalil, R.; Cosa, G. *Can. J. Chem.* **2011**, *89*, 385–394.
(37) Loudet, A.; Burgess, K. *Chem. Rev.* **2007**, *107*, 4891–4932.
(38) Pecher, J.; Guenoun, P.; Chevallard, C. *Cryst. Growth Des.* **2009**, *9*, 1306–1311.
(39) Lopez Arbeloa, F.; Banuelos, J.; Martinez, V.; Arbeloa, T.; Lopez Arbeloa, I. *Int. Rev. Phys. Chem.* **2005**, *24*, 339–374.
(40) Wood, T. E.; Thompson, A. *Chem. Rev.* **2007**, *107*, 1831–1861.
(41) Haugland, R. P. *Handbook of Fluorescent Probes and Research Products*, 10th ed.; Molecular Probes, Inc.: Eugene, OR, 2005.
(42) Mori, H.; Boker, A.; Krausch, G.; Muller, A. H. E. *Macromolecules* **2001**, *34*, 6871–6882.
(43) Ohno, K.; Morinaga, T.; Koh, K.; Tsujii, Y.; Fukuda, T. *Macromolecules* **2005**, *38*, 2137–2142.
(44) Behling, R. E.; Williams, B. A.; Staade, B. L.; Wolf, L. M.; Cochran, E. W. *Macromolecules* **2009**, *42*, 1867–1872.
(45) Pincus, P. *Macromolecules* **1991**, *24*, 2912–2919.
(46) Degennes, P. G. *Macromolecules* **1980**, *13*, 1069–1075.
(47) Kurosawa, S.; Aizawa, H.; Talib, Z. A.; Atthoff, B.; Hilborn, J. *Biosens. Bioelectron.* **2004**, *20*, 1165–1176.
(48) Dong, R.; Krishnan, S.; Baird, B. A.; Lindau, M.; Ober, C. K. *Biomacromolecules* **2007**, *8*, 3082–3092.
(49) Tsarevsky, N. V.; Pintauer, T.; Matyjaszewski, K. *Macromolecules* **2004**, *37*, 9768–9778.
(50) Witte, K. N.; Kim, S.; Won, Y.-Y. *J. Phys. Chem. B* **2009**, *113*, 11076–11084.
(51) Zhulina, E. B.; Birshtein, T. M.; Borisov, O. V. *Macromolecules* **1995**, *28*, 1491–1499.
(52) Konradi, R.; Ruhe, J. *Macromolecules* **2005**, *38*, 4345–4354.
(53) Arbeloa, F. L.; Prieto, J. B.; Martínez, V. M.; López, T. A.; Arbeloa, I. L. *ChemPhysChem* **2004**, *5*, 1762–1771.
(54) Krumova, K.; Cosa, G. *J. Am. Chem. Soc.* **2010**, *132*, 17560–17569.